

# A Numerical Investigation of Different Behavioral Regimes of the Free-Falling Solid Objects in Laponite Suspension

H. Koochi, N. Maleki-Jirsaraei<sup>†</sup> and S. Azizi

*Complex Systems Laboratory, Physics Department, Alzahra University, Tehran, P.O. Box 1993891176, Iran*

<sup>†</sup>*Corresponding Author Email: maleki@alzahra.ac.ir*

(Received February 15, 2019; accepted June 18, 2019)

## ABSTRACT

In this paper, we have numerically examined models that are capable of describing free falling regimes of a rigid sphere in a thixotropic fluid as Laponite. By simultaneously solving the dynamical equations governing both sphere and fluid systems, different regimes referred to in the experimental methods, are obtained. Three common behavioral regimes are: i) quickly stopping object, ii) fall with decreasing velocity, and iii) falling with a constant velocity in a steady-state mode. The initial state of the fluids (which is a function of the aging time), the characteristic relaxation time of microstructure's building up under shear, the characteristic thickness of the yielded zone around the sphere, and critical yield stress value besides the diameter and density of the sphere are effective parameters that change the regime.

**Keywords:** Free falling; Thixotropy; Aging time; Yield stress; Drag force; 4th Runge-kutta method.

## NOMENCLATURE

$a$	coefficient in Herschel–Bulkley model	$\beta$	parameter related to the fluid species
$b$	coefficient in Herschel–Bulkley model	$\dot{\gamma}$	shear rate
$F_d$	drag force	$\dot{\gamma}_c$	critical shear rate
$F_y$	yield stress force	$\dot{\gamma}_{ss}$	steady state shear rate
$F_{y_0}$	initial yield stress force	$\theta$	relaxation time
$g$	gravitational acceleration	$\kappa$	coefficient
$k_c$	coefficient of yielding volume surface	$\lambda$	microstructural parameter
$L$	characteristic thickness of shear	$\lambda_0$	initial microstructural parameter
$m$	mass	$\lambda_{ss}$	steady state microstructural parameter
$n$	parameters related to the fluid species	$\mu$	viscosity
$R$	radius	$\mu_0$	limiting viscosity
$S$	yield volume surface	$\rho_f$	density of the fluid
$T$	stress tensor	$\rho_s$	density of the sphere
$t$	time	$\sigma$	shear stress
$t_{age}$	aging time	$\sigma_{ss}$	steady state shear stress
$V$	velocity	$\sigma_y$	yield stress
$u$	velocity vector	$\sigma_{y_0}$	initial yield stress
$\eta$	complex viscosity	$\tau$	stress growth exponent in the unit of time
$\alpha$	parameter related to the fluid species		

## 1. INTRODUCTION

The free falling of solid objects through non-Newtonian fluids is a simple and suitable method for a fundamental understanding of the flow characteristics. It is also useful for optimizing industrial processes involving particle sedimentation. In thixotropic suspensions, the dependency of the rheological properties on time and shear rate causes a very complex settling problem. Thixotropic behavior in a fluid refers to the competition between breaking down the fluid microstructure under shear and forming the microstructure at the rest state (Møller *et al.*, 2006; Coussot *et al.* 2002a). Laponite belongs to this category of fluids. In fact, in addition to thixotropy, it also exhibits shear thinning, yield stress, and viscoelastic behavior.

Particles settling in Laponite has been reported to exhibit amazing motion regimes (Fazilati *et al.*, 2017; Ferroir *et al.*, 2004; Bonn *et al.*, 2002). In a simplistic look at the issue of free fall, especially in Newtonian fluids, two regimens are expected to emerge one including a steady state fall with a constant velocity and the other one a fall that quickly ends up to rest and causes the settling object almost suspended on the surface of the fluid. These two expected results come from a balance between the apparent weight and the drag force experienced by the settling object. For the first time, Ferroir *et al.* (2004) showed that, based on the initial state of Laponite which is a function of its aging time, a third regime also occurred which was hard to explain at first. They prepared a suspension of Laponite and left it at different times to age and then dropped a solid sphere such that it can settle under gravity in the fluid. In addition to the two regimes mentioned above, also, a continuously decreasing velocity regime was observed at intermediate aging times. In their opinion, thixotropy was the principal factor to control the motion. They argued that a bifurcation process similar to the viscosity bifurcation in an inclined plane experiment for thixotropic fluids might have taken place (Ferroir *et al.* 2004; Coussot *et al.* 2002a & 2002b).

Later, Tabuteau *et al.* (2007a) & (2007b), confirmed the three regimes mentioned above for both Carbopol and Laponite gel, depending on the characteristics of the solid sphere. The Carbopol gel they used exhibit yield stress properties but not thixotropic, unlike Laponite. They verified that only a very thin layer of the fluid around the solid object was subjected to shear stress, and the rest of the fluid was deformed elastically. Also, the thickness of the fluidized region in simple yield stress fluid could be 100 orders of magnitude larger than in thixotropic yield stress fluids.

In another interesting work, Hasani *et al.* (2011) and Fazilati *et al.* (2017), experimentally studied the free falling motion of a sphere in Laponite suspension and noticed a pseudo-oscillatory regime for certain range of aging time and diameter of the sphere. Due to the complexity of Laponite, the

origin of this peculiar behavior is still unclear.

As far as we are aware of, based on published data the free fall of a solid object in Laponite has only been investigated experimentally. In fact, the lack of a proper theoretical analysis to predict and formulate the various observed regimes is quite evident in this area. So, the aim of this article is to predict the behavioral regime of a solid sphere settling in a thixotropic yield stress fluid such as Laponite by numerically solving the dynamic equations governing the whole system comprising the fluid and the solid.

## 2. MATERIALS AND METHODS

The stress exerted on a thixotropic fluid while a solid particle is settling within it constantly changes the fluid's microstructure and thereby the particle's dynamics due to a change in the fluid's viscosity and/or yield stress. So, it is obviously a challenging fluid mechanics problem, which is a formidable task. Some simplifications are therefore needed to make the analysis tractable.

### 2.1 Mathematical Formulation of Laponite's Structure

When a thixotropic fluid is subjected to shear stress and then left to rest, the internal bounds broken down by shear start rebuilding in time until an equilibrium is reached. In other words, the fluid microstructure rejuvenates under shear and ages at rest. The competition between rejuvenation and aging determines the viscosity of the fluid that is a function of time and imposed shear stress (Møller *et al.*, 2006; Shahin *et al.*, 2012). If the applied stress is smaller than a critical value, viscosity increases in time and the shear rate reaches zero at rest. But, in large enough shear stress (greater than a critical value), viscosity decreases in time and therefore the fluid flows with much larger shear rate rather than predicted shear rate by simple yield stress models. Such phenomena, known as *viscosity bifurcation*, suggests that the material is simultaneously thixotropic and viscoplastic. Accordingly, Coussot *et al.* (2002b) modified Moore's model (which applies to thixotropic materials) such that it can describe the dynamical behavior of thixotropic materials exhibiting yield stress. The model is typical of generalized Newtonian fluid models (GNFs) with the only difference being that the viscosity is time-dependent in addition to being shear-dependent. A structural parameter,  $\lambda$ , determines the degree of restructuring of the microstructures within the fluid, which satisfies the following kinetic equation Coussot *et al.* (2002b):

$$\frac{d\lambda}{dt} = \frac{1}{\theta} - \alpha\lambda\dot{\gamma} \quad (1)$$

where  $\theta$  is the relaxation time parameter (which refers to the characteristic time for microstructure rebuild while at rest). In the model proposed by Coussot *et al.* (2002b) fluid's viscosity is related

to the structural parameter in one of the two following forms with the first form being more common:

$$\mu = \mu_\infty(1 + \beta\lambda^n) \quad (2)$$

$$\mu = \mu_\infty e^{\beta\lambda} \quad (3)$$

where  $a$ ,  $\beta$ , and  $n$  are the parameters related to any specific fluid. In these equations,  $\mu_\infty$  refers to the limiting viscosity at very high shear rates where the microstructure is totally destroyed and we have  $\lambda = 0$  (Møller *et al.*, 2006; Coussot *et al.* 2002b). Generally, at high shear rates, the fluid reaches a steady state where  $d\lambda/dt = 0$ , and so the steady flow curve becomes (Møller *et al.*, 2006):

$$\sigma_{ss} = \dot{\gamma}_{ss} \mu_\infty (1 + \beta / (\alpha \theta \dot{\gamma}_{ss})^n) \quad (4)$$

If  $d\sigma_{ss}/d\dot{\gamma}_{ss} = 0$  and  $n \geq 2$ , then the sign of the viscosity around a critical shear rate changes. In the case of  $n = 2$ , the critical shear rate is equal to  $\dot{\gamma}_c = \sqrt{\beta/\alpha\theta}$  and for smaller shear rates than  $\dot{\gamma}_c$ , the viscosity is negative which means an instability appearing in the fluid (Møller *et al.*, 2006).

## 2.2 Mathematical Formulation of the Free Falling of a Solid Object

The net forces applied to a settling object should be large enough to flow the fluid and move object inside it. Basically, in a yield stress fluid, the imposed shear stress caused by the solid object must overcome the critical yield stress of the fluid. The accurate yield stress concept and the amount that an object experience is a complex topic which still is not exactly defined (Møller *et al.*, 2006; Barnes *et al.*, 1985; Coussot, 2014; Bonn *et al.*, 2017). In accordance with a modified power-law model of Herschel–Bulkley fluids, the yield stress part,  $\sigma_y$ , could be an implicit function of time as follows (Beaulne and Mitsoulis, 1999):

$$\sigma = \sigma_y (1 - \exp(-\tau\dot{\gamma})) + b\dot{\gamma}^n \quad (5)$$

where  $\tau$  is the stress growth exponent in the unit of time. The other important force playing a key role is called the drag force, which is a function of the velocity of the object and the viscosity of the fluid. Generally, the drag force of a yield stress fluid is calculated in the following equation (Ferroir *et al.*, 2004):

$$F_d = \int_S (T \cdot n) u dS \quad (6)$$

in which  $S$  is the surface of the yielding volume around the object;  $T$  is the stress tensor;  $n$  is the outer normal vector at any point on the surface  $S$ ; and  $u$  is the velocity vector (Ferroir *et al.*, 2004). However, calculating the drag force in thixotropic yield stress fluids appears to be much more complicated and it has not yet been properly modeled. In the literature, simplified empirical relationships have been proposed for this purpose

(Gumulya *et al.*, 2014; Wachs *et al.*, 2016). For instance, Ferroir *et al.* (2004) modified the Stokes' law for thixotropic fluids lacking yield stress as follows:

$$F_d = 6\pi R V \mu_\infty (1 + \beta\lambda^n) \quad (7)$$

where  $V$  and  $R$  are respectively the velocity and radius of the settling sphere. For thixotropic fluids showing yield stress, based on experimental data for Laponite gel (obtained under creeping-flow conditions) Tabuteau *et al.* (2007a) suggested the following equation for the drag force:

$$F_d = F_y(t_{age})(a + b\dot{\gamma}^n) \quad (8)$$

where  $a$ ,  $b$  and  $n$  are fluid parameters and  $F_y(t_{age})$  is a stress-induced yielding force modeled as:

$$F_y(t_{age}) = 4\pi R^2 k_c \sigma_y(t_{age}) \quad (9)$$

where  $k_c$  is the coefficient of yielding volume surface,  $\sigma_y$  being the fluid's yield stress and  $t_{age}$  is the aging time. That is to say that, the role of the thixotropy of Laponite gel appears in the yield stress part of the drag force through allowing it to be a function of the aging time (Tabuteau, Oppong, Bruyn and Coussot, 2007).

## 2.3 Numerical Method

The solid sphere and the fluid are two dependent systems that dynamically interact with each other. Therefore, the differential equations governing the spherical object and the fluid system are coupled and should be solved simultaneously. To that end, in the present work, we intend to use both experimentally proposed models by Tabuteau *et al.* (2007a) and Ferroir *et al.* (2004) and compared the result of the numerical solving with the experimental results for specified parameters in the referred papers (Ferroir *et al.*, 2004; Tabuteau, Oppong, Bruyn and Coussot, 2007). In addition, we have also solved the equations governing the sphere-fluid coupled system in a general model with respect to both the net force applied to the sphere and the fluid's thixotropic behavior.

Firstly, based on the Tabuteau *et al.* (2007a) model, the only differential equation governing the sphere becomes:

$$\frac{dV}{dt} = \frac{(\rho_s - \rho_f)g}{\rho_s} - \frac{3k_c \sigma_y(t_{age})(a + b\dot{\gamma}^n)}{\rho_s R} \quad (10)$$

where  $\rho_s$  is the density of the sphere (radius =  $R = R_{min}$ ),  $\rho_f$  is the density of the fluid.

Secondly, according to the proposed model by Ferroir *et al.* (2004), at each moment the sphere deals with fresh fluid. That is to say that, only a slight domain of depth,  $H$ , around the sphere is fluidized during settling. The system of coupled differential equations to be solved simultaneously are as follows:

$$\frac{dV}{dt} = \frac{(\rho_s - \rho_f)g}{\rho_s} - \frac{9V \mu_\infty(1 + \beta\lambda^2)}{2\rho_s R^2} \quad (11)$$

$$\frac{d\lambda}{dt} = \frac{1}{\theta} + \left(\frac{1}{H}(\lambda_0 + \frac{t}{\theta}) - (\frac{\alpha}{L} + \frac{1}{H})\lambda\right)V$$

where  $\lambda_0$  shows the initial state of the fluid's microstructure and  $L$  refers to the characteristic length of the fluid around the sphere, which is affected by the fall. Thirdly, in a general model, we need to consider the dynamic of the sphere's velocity and the fluid's microstructure as two combined differential equations as follow:

$$\frac{dV}{dt} = \frac{\Delta mg}{m} - \frac{F_y}{m} - \frac{F_d}{m} \quad (12)$$

$$\frac{d\lambda}{dt} = \frac{1}{\theta} - \lambda\alpha \frac{V}{2R}$$

which  $F_y$ , is the force generated by the yield stress properties of the fluid and changes exponentially as:

$$F_y = 4\pi R^2 \sigma_{y0} \exp(-\kappa V / 2R) \quad (13)$$

Choosing the right amount of the initial yield stress,  $\sigma_{y0}$ , is a challenging matter. Here, by considering spheres of different radii that are released from the free surface of the fluid without an initial velocity, the value of  $\sigma_{y0}$  is calculated from almost equality of the  $F_y$  and the apparent weight,  $\Delta mg$ , for the smallest radius. Which means that even the smallest sphere, could overcome the yield stress or in another word,  $\sigma_{y0}$  adopted as the critical yield stress, that is a characteristic property of the fluid and constant for all larger radii and non-zero initial sphere's velocity:

$$\sigma_{y0} \cong \frac{4}{3} g R_{\min} (\rho_s - \rho_f) \quad (14)$$

Since the drag force,  $F_d$ , is a function of fluid's microstructure through the viscosity, therefore by considering Eqs. (2) and (3) two simple form of modeled drag force exerted on the sphere are:

$$F_d = 6\pi R V \mu_\infty (1 + \beta\lambda^2) \quad (15)$$

$$F_d = 6\pi R V \mu_\infty e^{\beta\lambda} \quad (16)$$

We eventually put  $F_y$  and  $F_d$  based on Eqs. (13), (15) and (16) on Eq.(12) and have numerically investigated time variations of both the sphere's velocity and the fluid's microstructure.

Here in this work, the sphere-fluid equations system of Eqs.(10) and (11) and couples system of Eq. (12) using Eqs. (13),(14),(15) or(16) were solved in one dimension (vertically) for a fluid column of selected heights (based on the model) and neglected effect of walls. The initial velocity of the sphere is a function of its height that releases relative to the free surface of the fluid which is referred to in the next section with more detail. The initial state of the fluid

microstructure is  $\lambda_0 = 1$ .

To solve the above system of differential equations, we rely on the 4<sup>th</sup>-order Runge-Kutta method and Fortran 90 programming language.

### 3. RESULTS AND DISCUSSION

#### 3.1 H. Tabuteau *et al.* Model

In this section, based on Eq. (10), we investigated a sphere's free-falling motion in a vessel of Laponite with a height of  $45\text{cm}$  and  $\rho_f = 1012\text{Kg}/\text{m}^3$ . A sphere of radius  $R = 1.99\text{cm}$  assuming to drop from a height of  $1\text{cm}$  above the fluid; its initial velocity at the free surface of the fluid is  $44\text{ cm/s}$ . Other chosen parameters are:  $a=0.93$ ;  $b=1$ ;  $n=0.5$ ;  $k_c=1.085$ ; and  $\sigma_y = 45\text{Pa}$  for  $t_{age} = 4\text{min}$  which is extracted from Tabuteau, Oppong, Bruyn and Coussot (2007).

We have examined the different characteristic length of the fluidized layer around the sphere for a constant  $\Delta\rho = \rho_s - \rho_f = 1589\text{Kg}/\text{m}^3$ . As can be seen in Fig. 1, where the sphere moves into the fluid of  $L \geq 0.3R$  :

- 1- For the small thickness of  $L$ , there was no movement in the fluid.
- 2- Increasing  $L$ , very quickly reduced the velocity and then a quick steady state was obtained.
- 3- The larger  $L$  led to the larger steady-state's velocities but not at a sharp rate. Larger steady state's velocity means a shorter falling time of reaching to the bottom of the vessel.

In Fig. 2,  $L = 1.009R$  for different value of  $\Delta\rho$  and it can be seen that:

- 1- An increasing velocity motion was observed for a large enough sphere's density.
- 2- For the smaller value of  $\Delta\rho$ , the velocity decreased till reached a steady state. More decreasing of  $\Delta\rho$ , only causes more abruptly and faster decreasing and lower value of steady-state's velocity.
- 3- For the very small value of  $\Delta\rho$ , the sphere stops immediately.

A different value of  $L$  shows similar trend depending on the range of the density. As mentioned, an increasing velocity regime took place in so large amount of  $\Delta\rho$  where the drag force and the yield stress are negligible compared to the apparent weight. Also, if  $\sigma_y(t_{age})$  reaches zero, the velocity will be increased for any value of  $\Delta\rho$ . It should be noted that a slow-moving behavior which suspends the sphere in the fluid, can not be seen in this model. According to the height of the fluid, the sphere eventually reaches the end of the vessel, though at very low steady-state velocity. In summary, we obtained that numerical solution of Eq. (10) does not verify the experimental result of

Tabuteau *et al.* (2007a), may be due to the failure to follow Laponite's flow-curve from Herschel-Bulkley's model.

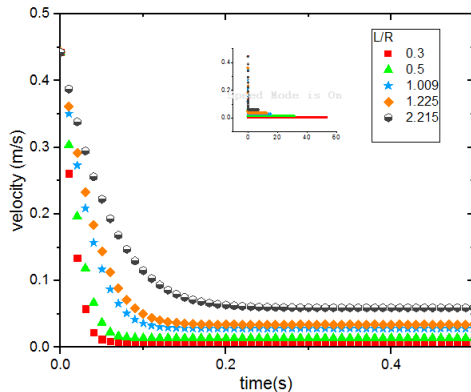


**Fig. 1.** Changes in sphere's velocity with time for different  $L/R = 0.3, 0.5, 1.009, 1.225, 2.215$  in Tabuteau *et al.* (2007a) model. Here  $\Delta\rho = 1589 \text{ Kg/m}^3$ . The inset shows variation until the sphere reaches the end of the vessel.

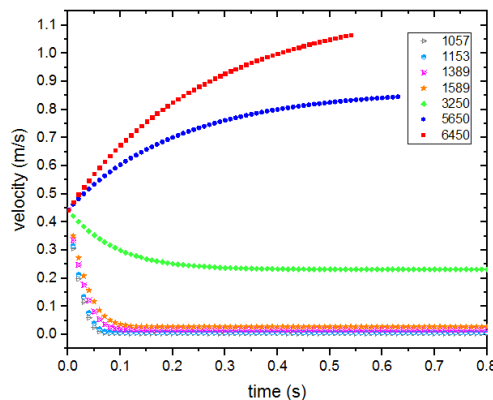


**Fig. 2.** Changes in the sphere's velocity with time for different  $\Delta\rho = 1057, 1153, 1389, 1589, 3250, 5650, 6450 \text{ Kg/m}^3$  in Tabuteau *et al.* (2007a) model. Here  $t_{age} = 4 \text{ min}$  and the thickness of the fluidized layer around the sphere is  $1.009R$ .

### 3.2 T. Ferroir *et al.* Model

Numerical solution of the coupled Eq. (11) for an iron spherical object of  $R=1.55 \text{ mm}$  and  $\rho_s = 7780 \text{ Kg/m}^3$ ; with an initial velocity of  $1 \text{ cm/s}$  which dropped freely inside a column of Laponite gel with heights of  $21 \text{ cm}$  and  $\rho_f = 1017 \text{ Kg/m}^3$ ; suggested that the characteristic time of relaxation time,  $\theta$ , plays a decisive role on the motion behavior. Fix characteristic parameters related to dynamical changes of  $\lambda$  assume as  $L = 2R, H = 6R, \lambda_0 = 1, \mu_0 = 1 \text{ Pa.s}, \alpha = 1$ , and  $\beta = 1$  but  $\theta$  varies from  $0.1 \text{ s}$  to  $50 \text{ s}$ . The result in Fig. 3 is shown that:

- 1- For a small value of  $\theta$ , about  $0.1 \text{ s}$ , the sphere stopped as soon as it dropped.

- 2- For a smaller value of  $\theta$  than  $10 \text{ s}$ , a decreasing velocity regime observed.

- 3- If  $\theta$  be as large as the  $50 \text{ s}$  a steady state regime happened.

Since the experimental results were shown that quickly stopping regime took place in a long amount of  $t_{age}$  and here in short  $\theta$ ; and also in the opposite, the steady state regime took place in a short amount of  $t_{age}$ , and here in long  $\theta$ ; thus the characteristic time of relaxation,  $\theta$ , should be inversely related to the aging time (Ferroir *et al.*, 2004). Investigation of the effect of  $\lambda_0$  for constant  $\theta$  also suggested that:

- 1- In loose initial microstructure, a steady state regime observed.

- 2- In strong enough  $\lambda_0$ , the sphere's motion stopped from the beginning.

- 3- A decreasing velocity regime observed for the intermediate  $\lambda_0$ .

Therefore, as a result, we argued that a longer aging time before settling, is equivalent to a larger initial state of  $\lambda_0$ , and as well, a longer amount of  $\theta$  after settling means a larger value of  $\lambda$  at any moment of the time.

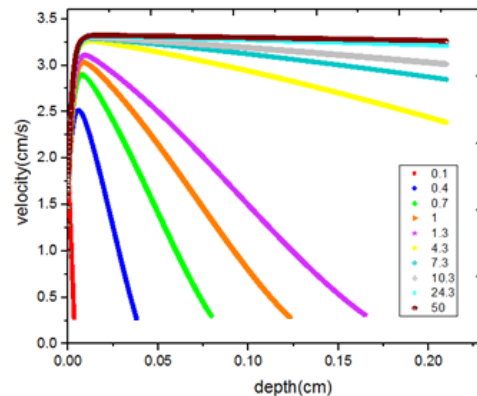


**Fig. 3.** Changes in velocity with depth for different  $\theta = 0.1, 0.4, 0.7, 1, 1.3, 4.3, 7.3, 10.3, 24.3$  and  $50 \text{ s}$ , in T. Ferroir *et al.* model.

### 3.3 A Coupled Fluid and Solid Object System

In this section, we report the result and detail of solving the generally coupled Eq. (12) in two forms by using Eqs. (13), (14), (15) or (16). Constant parameters are:  $\rho_s = 7000 \text{ Kg/m}^3, \sigma_{y0} = 117 \text{ N/m}^2, \kappa = 0.001 \text{ s}^{-1}, n = 2$ ; and the value of rest parameters all are unit. Calculations repeated for different radii of the sphere and two initial velocities: zero and  $44 \text{ cm/s}$  respectively for a sphere released from the free surface of the fluid and from  $1 \text{ cm}$  above it. Also, both models of viscosity formulation of the drag force examined as Eqs. (15) and (16). We defined

the height of the fluid's column large enough and a function of time and taken the time long enough so that the sphere could experience all the regimes.

In Figs. 4 to 6 is shown three regimes for a radius variation:

- 1- For a small radius about  $2.5\text{mm}$ , the motion rapidly stopped.
- 2- For radii larger than  $2.5\text{mm}$  to  $2.85\text{mm}$ , a decreasing velocity regime observed which the sphere stopped finally.
- 3- More large radii motion reached to a steady state regime where the sphere moved with a constant velocity.

Selecting different values for the initial velocity or changing the viscosity relationship according to Eq. (2) or (3), only affected the velocity value at any moment but it did not switch the regime. We noticed that in decreasing velocity regime before the sphere stops completely, the velocity grows up. It seems, that this suddenly rising mode of the velocity had no physical meaning and probably was related to some numerical instability of running the Fortran 90 code of RK4 methods, and velocity finally reached to zero as it is shown in Fig. 7.

Therefore, comparing with scientific literature, we can say that this general model is capable of qualitatively predicting the three experimentally reported regimes (Ferroir *et al.*, 2004; Tabuteau, Oppong, Bruyn and Coussot, 2007). But due to the main role of the fluid's aging time affecting the settling (which is not defined in the system of equations), the velocity can not quantitatively be compared.

In Fig. 8 it can be seen how the structural parameter,  $\lambda$ , changes with time. When the velocity decreased,  $\lambda$  increased and conversely. Also, when the velocity of the sphere reaches a steady state, the dynamical variation of  $\lambda$  is equalized zero and microstructure indicates a stable steady state.

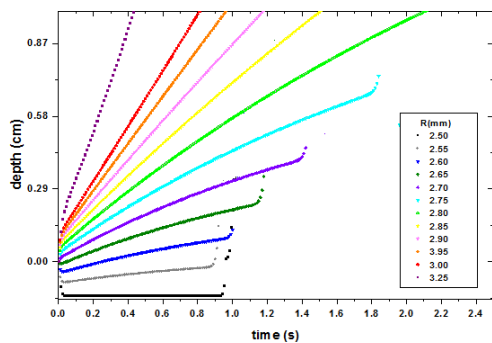


**Fig. 4.** Changes in depth of the sphere with time for different radii. Here  $V_0 = 44\text{ cm/s}$  and the viscosity follows Eq. (3).

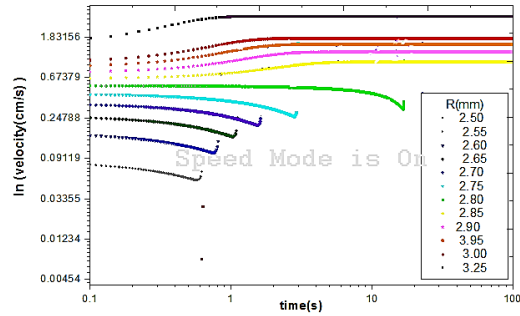


**Fig. 5.** Changes in the velocity with time for different radii without initial velocity. Here the viscosity follows Eq. (2).

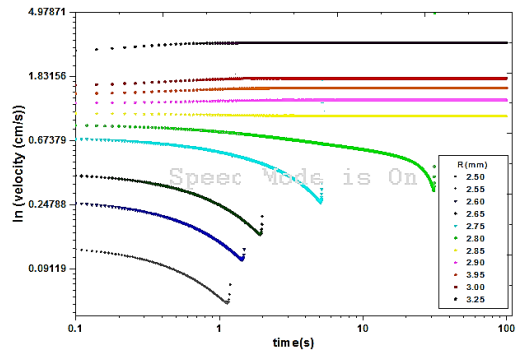


**Fig. 6.** Changes in the velocity with time for different radii. Here  $V_0 = 44\text{cm/s}$  and the viscosity follows Eq. (2)

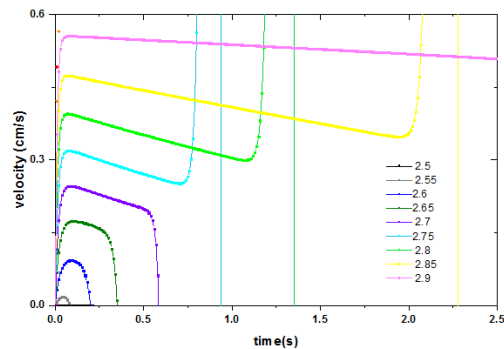


**Fig. 7.** Changes in the velocity with time for different radii without initial velocity. Here the viscosity follows Eq. (3).

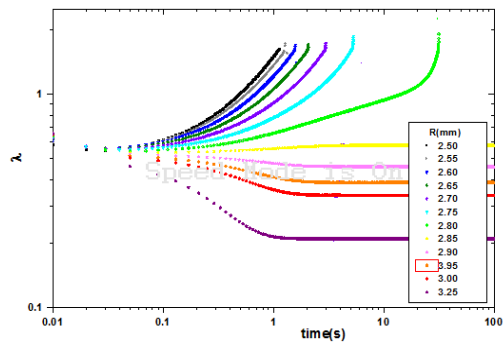


**Fig. 8.** Changes in the structural parameter,  $\lambda$ , with time for different radii. Here  $V_0 = 44\text{ cm/s}$  and the viscosity follows Eq. (2).

#### 4 FUTURE IDEA

The irregular oscillating motion has been observed in [Hasani \*et al.\* \(2011\)](#) and [Fazilati \*et al.\* \(2017\)](#) experimental tests, is one of the most amazing regimes of the free falling sphere in Laponite gel. Here we played a bit with experimental data of [Fazilati \*et al.\* \(2017\)](#) and have obtained the flow curve of the fluid around the sphere due to its pseudo-oscillatory motion, and then compared it with the flow curve of Laponite gel which [Fazilati \*et al.\* \(2017\)](#) derived from the rheological test. It was determined that in a certain range of shear rates (in the shear stress control rheological test) the viscosity of the fluid becomes negative (in equivalent to the slope of the flow curve), that it is to say an unknown instability took place in the fluid ([Fielding, 2016](#); [Maki and Renardy, 2012](#); [Cheng, 2003](#)). As can be seen in Fig. 9, the flow curve caused by the settling of the sphere and the unstable branch of the flow curve caused by the rheology test of laponite, both occur in the same range of shear rates. Therefore, may it can be said that reaching to a certain range of shear rates are causing instability and the reason for the pseudo-oscillatory motion of the sphere is due to the occurrence of instability in the fluid. Considering the structural model of  $\lambda$  for thixotropic fluids (Eq. (4)) which predicts an unstable steady state, may lead us to model and analytically understand the cause of the fluctuation in the sphere's velocity ([Moller, 2008](#)). In the next works, we will try to explain and model the pseudo-oscillation settling using a suitable numerical method which can predict the instability ([Bönisch \*et al.\*, 2007](#); [Jenny \*et al.\*, 2017](#)).

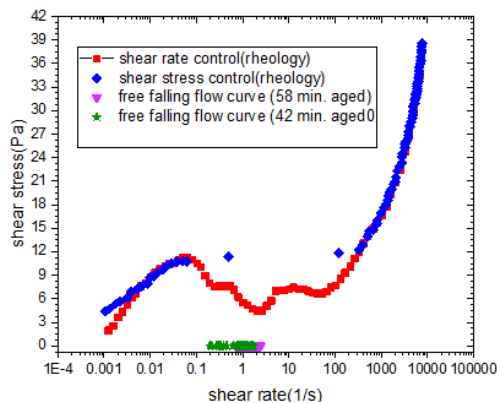


**Fig. 9. Flow curve of Laponite gel: (—■) shear rate control from  $10^{-3} \text{ s}^{-1}$  to  $10^4 \text{ s}^{-1}$  in 71 steps of 5s duration and (◆) Shear stress control from 0 to 40Pa in 80 steps of 5s duration ([Fazilati \*et al.\*, 2017](#)), flow curve of fluid due to falling a sphere of  $R=1.01\text{mm}$  in Laponite suspension: (▼) with an aging time of 58min, and (★) with an aging time of 42min.**

#### 5 CONCLUSION

In conclusion, when a spherical solid sphere falls under the gravity into the Laponite gel, based on

experimental background, four regimes for velocity variation have been seen ([Fazilati \*et al.\*, 2017](#)). Here we numerically investigated and modeled three common regimes. The initial state of the fluid's microstructure,  $\lambda_0$ , aging time and the characteristic relaxation time of the fluid,  $\theta$ , alongside the size and density of the sphere control behavioral regimes of free falling. We noticed that aging time and  $\theta$  play an opposite impact on the sphere movement. The thickness of the fluid layer around the sphere which affected by the stress field induced by the object,  $L$ , also played a fundamental role in the fluid and object interaction and need further study to determine its exact amount. Therefore, choosing a perfect combination of these four major quantities:  $\sigma_y$ ,  $\lambda_0$ ,  $\theta$ , and  $L$ , is very influential on how the sphere moves and the velocity changes.

In summary, for a thixotropic yield stress fluid we numerically observed these regimes as follow:

- 1- In the same initial state fluids, the motion of a sphere with a small radius or density quickly stopped. Also for a constant sphere, a fluid with small characteristic relaxation time,  $\theta$ , or fluid with a strong initial state of microstructure, made the sphere to stop fast as soon as it starts to move.
- 2- The next regime has been observed for spheres with large density or large radius in the same fluid's initial state, and also for same spheres in a fluid with weak microstructure or long  $\theta$ ; which the object fell in a steady state for both velocity and fluid's microstructure.
- 3- Intermediate size spheres in the same initial state fluids and also similar spheres in middle initial state fluid or mean  $\theta$ , have shown a decreasing velocity regime that ultimately stopped.
- 4- A pseudo-oscillating regime in particular mix-up of the aging time and solid object's size only reported in experimental references and not explained yet. However, we guessed that it is reasonably due to some instability in the microstructure of the fluid.

#### APPENDIX 1: LAPONITE, THE STRUCTURE, APPLICATIONS, AND RHEOLOGICAL BEHAVIOR

Laponite is a synthetic mineral clay that composed from nano-disk particles with highly negatively charged face (diameter about 25nm) and a positively charged rim (thickness about 0.92nm). Its crystalline structure consists of layered silicate similar to other clay minerals housing a central magnesium core between two silica sheets ([Tomás, H. \*et al.\*, 2018](#); [Cummins, . 2007](#)). A schematic representation of Laponite nanocrystal geometry and chemical structure is shown in Fig. 10.

When Laponite powder is dispersed in water, a colloidal suspension with different phases forms via swelling ([Tomás, \*et al.\*, 2018](#); [Cummins, . 2007](#);

Ruzicka, *et al.*, 2011; Bonn, *et al.*, 1999). Long-time Laponite phases discussed in literature incorporate liquid with clusters, Wigner glass, high-density gel or ‘house of cards’ structure, low-density gel and nematic phases (Laponite B). Growing a phase potentially depends on particles density, ionic strength, long or short range part of the electrostatic interactions and time of rest (aging time). In Fig. 11 the long-time Laponite phase diagram is reported in the ( $C_w$ ,  $C_s$ ) where  $C_w$  is clay concentration and  $C_s$  is salt concentration.

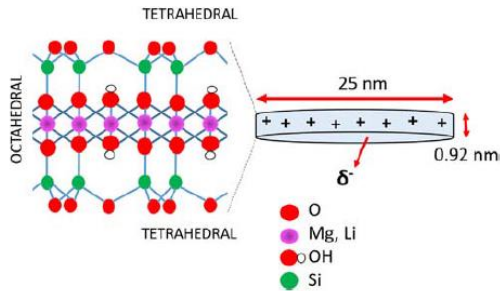


**Fig. 10. Schematic representation of Laponite nanocrystal geometry (disk-like) and chemical structure (Tomás, *et al.*, 2018).**

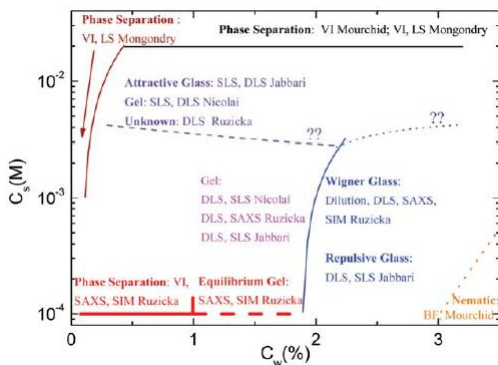


**Fig. 11. Long-time phase diagram of Laponite suspension (Ruzicka, *et al.*, 2011)**

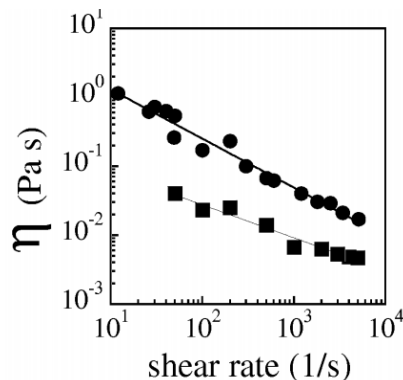


**Fig. 12. Complex viscosity versus shear rate for a 1.5 wt% (■) and 3.7 wt% (●) Laponite suspension (Abou, *et al.*, 2003).**

According to Bonn *et al.* (2002) experimentally

investigation of the role of aging and rejuvenation of Laponite, complex viscosity increases by increasing the aging time which refers to its thixotropic properties. Laponite gel is strongly thixotropic and the rate of restructuring depends on composition, electrolyte level, age of the dispersion, and temperature (Cummins, 2007; Ahlfeld, *et al.*, 2017). Laponite is extensively used as a rheological modifying or thixotropic agent in many liquid or suspension products found in agriculture, building, household, and personal care, surface coating, paper, and polymer film industries.

According to the rheological measuring tests of Fazilatie *et al.* (2017) which are shown in Fig. 9, by imposing the shear stress, at critical stress, there is a plateau region where a range of shear rates are inaccessible and a jump from the low shear rate (high viscosity) branch to the high shear rate (low viscosity) branch is observed. By imposing the shear rate, a Vander Waals-like loop with a part with a negative slope is observed that to say an instability flow appears in the fluid.

Abou *et al.* (2003) also measured the flow curve of a 1.5 wt% Laponite suspension, that is shown in Fig. 12. As can be seen, the viscosity decreases by increasing the shear rate, which is a sign of shear-thinning behavior of Laponite gel and characterized by a power law of viscosity:  $\eta \propto \dot{\gamma}^{0.6 \pm 0.1}$ . Due to strong shear-thinning properties of Laponite, it is well known as a rheological enhancer of polymeric solutions (Ahlfeld, *et al.* 2017). In addition, it is shown that Laponite is strongly viscoelastic, even at very low particle concentrations (Ahlfeld, *et al.* 2017; Mourchid, *et al.*, 1998).

In another work, Fall and Bonn (2012) exhibited a very strong shear thickening behavior of Laponite by addition of polyethylene oxide (PEO). Because of the shear thickening property, it is used in a number of applications such as cosmetics and paints (Ahlfeld, *et al.* 2017).

Commercially, Laponite RD and XLG are most common grades which Laponite RD is most frequently studied grade, is used in many household and industrial products including cleansers, surface coatings, and ceramic glazes. Laponite XLG is a high-purity grade of Laponite RD, processed to remove impurities such as heavy metals e.g. lead and arsenic. This grade is used in personal care and cosmetic products including shampoos and sunscreens (Cummins, H. Z. 2007).

## REFERENCES

- Abou, B., D. Bonn and J. Meunier (2003). Nonlinear rheology of Laponite suspensions under an external drive. *Journal of rheology* 979,47
- Ahlfeld, T., G. Cidonio, D. Kilian1, S. Duin, A. R. Akkineni, J. I. Dawson, S. Yang, A. Lode1, R. O. C. Oreffo and M. Gelinsky (2017). *Development of a clay-based bioink for 3D cell printing for skeletal application*. IOP Publishing Ltd

- Barnes, H. A. and K. Walters (1985). The yield stress myth?. *Rheol Acta*, 24, 323-326.
- Beaulne, M. and E. Mitsoulis (1999). Creeping motion of a sphere in tubes filled with Herschel–Bulkley fluids. *Journal of Non-Newtonian Fluid Mechanics* 72, 55-71.
- Bönisch, S. and V. Heuveline (2007). On the numerical simulation of the unsteady free fall of a solid in a fluid: I. The Newtonian case. *Computers & Fluids* 36(9), 1434-1445.
- Bonn, D., H. Kellay, H. Tanaka, G. Wegdam and J. Meunier (1999). Laponite: What Is the Difference between a Gel and a Glass?. *Langmuir* 15, 7534-7536
- Bonn, D., M. M. Denn, L. Berthier, T. Divoux and S. Manneville (2017). Yield Stress Materials in Soft Condensed Matter. *Review of Modern Physics* 89, 035005.
- Bonn, D., S. Tanase and B. Abou (2002) Laponite: Aging and Shear Rejuvenation of a Colloidal Glass. *Physical Review Letters* 89(1), 015701(1-4).
- Cheng, D. C. H. (2003). Characterization of thixotropy revisited. *Rheol Acta* 42, 372-382.
- Coussot, P. (2014). Yield stress fluid flows A review of experimental data. *Journal of Non-Newtonian Fluid Mechanics* 211, 31–49.
- Coussot, P., Q. D. Nguyen, H. H. Huynh and D. Bone (2002b). Viscosity bifurcation in thixotropic, yielding fluids. *Journal of Rheology* 46(3), 573-589
- Coussot, P., Q. D. Nguyen, H. T. Huynh and D. Bonn (2002a). Avalanche Behavior in Yield Stress Fluids. *Physical Review Letters* 88(17), 175501.
- Cummins, H. Z. (2007). Liquid, glass, gel: The phases of colloidal Laponite. *Journal of Non-Crystalline Solids* 353, 3891–3905
- Fall, A. and D. Bonn (2012). Shear thickening of Laponite suspensions with poly (ethylene oxide). *Soft Matter* 8, 4645–4651.
- Fazilati, M, N. Maleki-Jirsaraei, S. Rouhani and D. Bonn (2017). The quasi-periodic and irregular motion of a solid sphere falling through a thixotropic yield-stress fluid. *Applied Physics Express* 10, 117301.
- Ferroir, T., H. T. Huynh, X. Chateau and P. Coussot (2004). Motion of a solid object through a pasty thixotropic fluid. *Physics of Fluids* 16(3), 070-663.
- Fielding, S. M. (2016). Triggers and signatures of shear banding in steady and time-dependent flows. *Journal of Rheology* 60, 821.
- Gumulya, M. M., R. R. Horsley and V. Pareek (2014). Numerical simulation of the settling behavior of particles in thixotropic fluids. *Physics of Fluids* 26, 023102(1-16).
- Hasani, S., N. Maleki-Jirsaraei and S. Rouhani (2011). Irregular Motion of a Falling Spherical Object Through Non-Newtonian Fluid. *arXiv:1108.3427*.
- Jenny, M, S. K. Richter, N. Louvet, S. Kali-Lami, (2016). Shear-banding and Taylor-Couette instability in thixotropic yield stress Fluids. *arXiv:1603.00339v1*
- Maki, K. L. and Y. Renardy (2012). The dynamics of a viscoelastic fluid which displays thixotropic yield stress behavior. *Journal of Non-Newtonian Fluid Mechanics* 181-182, 30-50.
- Moller, P. (2008). *Shear banding and the solid/liquid transition in yield stress fluids. Ph. D. thesis, University Pierre et Marie Curie, Paris, France.*
- Møller, P. C. F., J. Mewis and D. Bonn (2006). Yield stress and thixotropy: on the difficulty of measuring yield stresses in practice. *Soft Matter* 2, 274-283.
- Mourchid, A., E. Le´colier, H. Van Damme and P. Levitz (1998). On Viscoelastic, Birefringent, and Swelling Properties of Laponite Clay Suspensions: Revisited Phase Diagram. *Langmuir* 14, 4718-4723
- Ruzicka, B and E. Zaccarelli (2011). A fresh look at the Laponite phase diagram. *Soft Matter* 7, 1268–1286
- Shahin, A. and Y. M. Joshi (2012). Physicochemical effects in aging aqueous laponite suspensions. *Langmuir* 28(44), 15674-15686
- Tabuteau, H., F. K. Oppong, J. R. de Bruyn and P. Coussot (2007a). Drag on a sphere moving through an aging system. *EPL*, 78, 68007.
- Tabuteau, H., P. Coussot and J. R. de Bruyn (2007b). Drag force on a sphere in steady motion through a yield-stress fluid. *Journal of Rheology* 51(125), 125-137.
- Tomás, H., C. S. Alves and J. Rodrigues (2018). Laponite®: A key nanoplatforms for biomedical applications?. *Nanomedicine: Nanotechnology, Biology, and Medicine* 14, 2420–2407
- Wachs, A. and I. A. Frigaard (2016). Particle settling in yield stress fluids: Limiting time, distance and applications. *Journal of Non-Newtonian Fluid Mechanics* 238, 189-204.